A STUDY OF TRANSIENT PHASE-CHANGE HEAT TRANSFER DURING CHARGING AND DISCHARGING OF THE LATENT THERMAL ENERGY STORAGE UNIT

Anica Trp, Kristian Lenic, Bernard Frankovic
Faculty of Engineering University of Rijeka, Vukovarska 58, HR-51000 Rijeka, Croatia
Phone: + 385 51 651 514, Fax: + 385 51 675 801, E-mail: anica.trp@riteh.hr

Latent thermal energy storage system of the shell-and-tube type with the phase change material (PCM) filling the shell side, which is used as a heat storage device in solar heating applications, has been analysed numerically and experimentally in this paper. The heat transfer in this type of thermal energy storage system is a conjugate problem of transient forced convective heat transfer between the heat transfer fluid (HTF) and the wall, heat conduction through the wall and solid-liquid phase-change of the PCM. Since phase-change heat transfer is non-linear due to the moving phase change boundary, analytical solutions are only known for a few problems with simple geometry and simple boundary conditions. Numerical methods provide a more accurate approach, so various techniques have been developed. Many authors [1] - [5] have used the enthalpy formulation, in which the energy equation for PCM is written in terms of enthalpy. A transient heat transfer phenomenon in a shell-and-tube latent thermal energy storage system has been studied numerically by Bellecci and Conti in [6] - [8], and numerically and experimentally by Lacroix in [9] and [10]. These authors have used an enthalpy method for solving phase-change heat transfer and employed standard empirical correlations to calculate convective heat transfer coefficient. Cao and Faghri in [11] and [12] have simulated numerically, using the temperature transforming model for phase-change heat transfer, the transient behaviour of the shell-and-tube thermal energy storage system employing a low Prandtl number HTF. Ismail and Abugderah in [13] have modelled numerically a phase change thermal energy storage system of the same type. In both papers, the transient HTF momentum and energy equations were solved simultaneously with the tube wall and the PCM energy equations, as one domain, in order to avoid the errors due to the use of empirical correlations. Zhang and Faghri in [14] have semi-analytically studied a shell-and-tube latent thermal energy storage system employing a moderate Prandtl number HTF. They concluded that the laminar forced convective heat transfer inside the tube never reaches a thermally developed state and must be solved simultaneously with the phase-change of the PCM, so the application of CFD methods is required. In [15] a transient phase-change heat transfer with conjugate forced convection in the shell-and-tube latent heat storage unit, with water as HTF and calcium chloride hexahydrate as PCM has been analysed numerically. In this paper, a transient heat transfer phenomenon during charging and discharging of the shell-and-tube latent thermal storage unit has been analysed numerically and experimentally. The mathematical model has been formulated. The enthalpy method for modelling phase-change heat transfer has been used. The dimensionless conservation equations for HTF, wall and PCM, with initial and boundary conditions, have been discretised by fully implicit control volume approach, that has been implemented in developed FORTRAN computer code, and solved simultaneously using an iterative procedure. Numerical model has been validated with experimental data. Series of numerical calculations have been performed in order to analyse transient phase-change heat transfer during charging and discharging of the latent thermal energy storage unit.

MATHEMATICAL MODEL OF TRANSIENT PHASE-CHANGE HEAT TRANSFER AND NUMERICAL SOLUTION

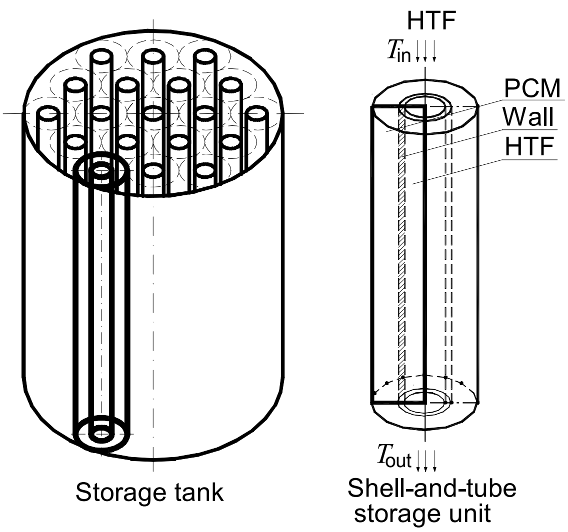

Fig. 1. Latent thermal energy storage system

The latent thermal energy storage system of the shell-and-tube type considered in the present study is shown in Fig. 1. The HTF is flowing by forced convection through the tubes. The PCM is filled in the shell space between the PCM container and the tubes. During charging of the system, hot fluid heats the PCM, the PCM melts and the heat is stored. During the discharging process, the PCM solidifies and the stored heat is delivered to the cold fluid. The tubes are arranged so that around each there is a boundary of region (dashed lines) in which the tube exchanges the heat with surrounding PCM. As a result, the shell and tube storage unit shown in Fig. 1, with adiabatic outer radius boundary condition, represents the physical system that has been analysed.

The mathematical model formulated to represent the transient behaviour of the physical system has been adequate to treat both melting and solidification processes. The following simplifications have been made:

- PCM is homogeneous and isotropic,
- HTF is incompressible and it can be considered as a Newtonian fluid,
- flow of the HTF is laminar, inlet velocity and inlet temperature of HTF are constant,
- initial temperature of the latent heat storage unit is uniform and PCM is in solid state for melting or in liquid state for solidification,
- HTF, tube wall and PCM temperature variations in angle direction are assumed to be negligible i.e. the problem is two-dimensional,
- the problem is axisymmetric,
- thermophysical properties of HTF, tube wall and PCM are constant,
- natural convection in the liquid phase of PCM has been ignored.

According to these simplifications, it follows that the computational domain is a bold framed part of the shell-and-tube storage unit shown in Fig. 1.

For expressing conservation equations in dimensionless form, following dimensionless parameters have been used:

$$R=\frac{r}{D_i},\ X=\frac{x}{D_i},\ W_X=\frac{w_x}{w_{in}},\ W_R=\frac{w_r}{w_{in}},\ P=\frac{p-p_0}{\rho_f\cdot w_{in}^2},\ \tau=\frac{w_{in}}{D_i}\cdot t,\ \mathrm{Re}=\frac{w_{in}\cdot D_i}{\upsilon_f},\ \mathrm{Pr}=\frac{\upsilon_f}{a_f},$$

$$\mathrm{Nu}=\frac{\alpha\cdot D_i}{\lambda_f},\ \Theta=\frac{T-T_m}{T_{in}-T_m}\ \text{(isothermal)},\ \Theta=\frac{T-T_{m\,min}}{T_{in}-T_{m\,min}}\ \text{(non-isothermal)},$$

$$\chi=\frac{H-\rho_s\cdot c_s\cdot T_m}{\rho_l\cdot q}\ \text{(isothermal)},\ \chi=\frac{H-\rho_s\cdot c_s\cdot T_{m\,min}}{\rho_l\cdot q}\ \text{(non-isothermal)},$$

$$\mathrm{St}=\frac{c_l\cdot(T_{in}-T_{m\,min})}{q}\ \text{(non-isothermal melting)},\ \mathrm{St}=\frac{c_s\cdot(T_m-T_{in})}{q}\ \text{(isothermal solidification)}.$$

The dimensionless continuity, momentum and energy equations, governing a transient two-dimensional heat transfer in the latent thermal energy storage unit, for incompressible, laminar fluid flow with no viscous dissipation, in a cylindrical coordinate system are as follows:

▪ for the HTF

$$\frac{\partial W_X}{\partial X}+\frac{1}{R}\cdot\frac{\partial\left(R\cdot W_R\right)}{\partial R}=0 \tag{1}$$

$$\frac{\partial W_X}{\partial\tau}+W_X\cdot\frac{\partial W_X}{\partial X}+W_R\cdot\frac{\partial W_X}{\partial R}=-\frac{\partial P}{\partial X}+\frac{1}{\mathrm{Re}}\cdot\left[\frac{\partial^2 W_X}{\partial X^2}+\frac{1}{R}\cdot\frac{\partial}{\partial R}\left(R\cdot\frac{\partial W_X}{\partial R}\right)\right] \tag{2}$$

$$\frac{\partial W_R}{\partial\tau}+W_X\cdot\frac{\partial W_R}{\partial X}+W_R\cdot\frac{\partial W_R}{\partial R}=-\frac{\partial P}{\partial R}+\frac{1}{\mathrm{Re}}\cdot\left[\frac{\partial^2 W_R}{\partial X^2}+\frac{1}{R}\cdot\frac{\partial}{\partial R}\left(R\cdot\frac{\partial W_R}{\partial R}\right)-\frac{W_R}{R^2}\right] \tag{3}$$

$$\frac{\partial\Theta_\mathrm{f}}{\partial\tau}+W_X\cdot\frac{\partial\Theta_\mathrm{f}}{\partial X}+W_R\cdot\frac{\partial\Theta_\mathrm{f}}{\partial R}=\frac{1}{\mathrm{Re\cdot Pr}}\cdot\left[\frac{\partial^2\Theta_\mathrm{f}}{\partial X^2}+\frac{1}{R}\cdot\frac{\partial}{\partial R}\left(R\cdot\frac{\partial\Theta_\mathrm{f}}{\partial R}\right)\right] \tag{4}$$

▪ for the tube wall $$\frac{\partial\Theta_\mathrm{w}}{\partial\tau}=\frac{1}{\mathrm{Re\cdot Pr}}\cdot\frac{a_\mathrm{w}}{a_\mathrm{f}}\cdot\left[\frac{\partial^2\Theta_\mathrm{w}}{\partial X^2}+\frac{1}{R}\cdot\frac{\partial}{\partial R}\cdot\left(R\cdot\frac{\partial\Theta_\mathrm{w}}{\partial R}\right)\right] \tag{5}$$

▪ for the PCM $$\frac{\partial\chi_\mathrm{p}}{\partial\tau}=\frac{1}{\mathrm{Re\cdot Pr}}\cdot\frac{a_\mathrm{p}}{a_\mathrm{f}}\cdot\left[\frac{\partial^2\chi_\mathrm{p}}{\partial X^2}+\frac{1}{R}\cdot\frac{\partial}{\partial R}\left(R\cdot\frac{\partial\chi_\mathrm{p}}{\partial R}\right)\right] \tag{6}$$

where χ is the dimensionless enthalpy that is related to the temperature with equation $\Theta_\mathrm{p}=A_\mathrm{b}\cdot\chi_\mathrm{p}+B_\mathrm{b}$, where factors A_b and B_b for isothermal and non-isothermal phase change are:

▪ isothermal phase change: $A_\mathrm{b}=\frac{1}{\mathrm{St}}\cdot\frac{\rho_\mathrm{l}\cdot c_\mathrm{l}}{\rho_\mathrm{s}\cdot c_\mathrm{s}}$, $B_\mathrm{b}=0$ for $\chi_\mathrm{p}<0$;

$A_\mathrm{b}=0$, $B_\mathrm{b}=0$ for $0\le\chi_\mathrm{p}\le1$; $A_\mathrm{b}=\frac{1}{\mathrm{St}}$, $B_\mathrm{b}=-\frac{1}{\mathrm{St}}$ for $\chi_\mathrm{p}>1$;

▪ non-isothermal phase change: $A_\mathrm{b}=\frac{1}{\mathrm{St}}\cdot\frac{\rho_\mathrm{l}\cdot c_\mathrm{l}}{\rho_\mathrm{s}\cdot c_\mathrm{s}}$, $B_\mathrm{b}=0$ for $\chi_\mathrm{p}<0$;

$A_\mathrm{b}=\frac{1}{\mathrm{St}}\cdot\frac{\rho_\mathrm{l}\cdot c_\mathrm{l}\cdot\Delta T_\mathrm{m}}{\rho_\mathrm{s}\cdot c_\mathrm{s}\cdot\Delta T_\mathrm{m}+\rho_\mathrm{l}\cdot q}$, $B_\mathrm{b}=0$ for $0\le\chi_\mathrm{p}\le\frac{\rho_\mathrm{s}\cdot c_\mathrm{s}\cdot\Delta T_\mathrm{m}}{\rho_\mathrm{l}\cdot q}+1$; $A_\mathrm{b}=\frac{1}{\mathrm{St}}$,

$B_\mathrm{b}=\frac{1}{\mathrm{St}}\cdot\frac{\left(\rho_\mathrm{l}\cdot c_\mathrm{l}-\rho_\mathrm{s}\cdot c_\mathrm{s}\right)\cdot\Delta T_\mathrm{m}}{\rho_\mathrm{l}\cdot q}-\frac{1}{\mathrm{St}}$ for $\chi_\mathrm{p}>\frac{\rho_\mathrm{s}\cdot c_\mathrm{s}\cdot\Delta T_\mathrm{m}}{\rho_\mathrm{l}\cdot q}+1$, $\Delta T_\mathrm{m}=T_\mathrm{m\,max}-T_\mathrm{m\,min}$.

Initial and boundary conditions are as follows:

▪ initial condition, $\tau=0$

$$0<R\le0.5,\quad 0\le X\le L/D_\mathrm{i}\ \Rightarrow\ W_X=W_R=0$$

$$0<R<R_\mathrm{o},\quad 0\le X\le L/D_\mathrm{i}\ \Rightarrow\ \Theta_\mathrm{f}=\Theta_\mathrm{w}=\Theta_\mathrm{p}=\Theta_\mathrm{init}$$

▪ boundary conditions, $\tau>0$

inlet plane, $X=0$ $\quad 0<R<0.5\ \Rightarrow\ W_X=1,\ W_R=0,\ \Theta_\mathrm{f}=1$

$$0.5\le R\le R_\mathrm{w}\ \Rightarrow\ \frac{\partial\Theta_\mathrm{w}}{\partial X}=0$$

$$R_\mathrm{w}<R<R_\mathrm{o}\ \Rightarrow\ \frac{\partial\Theta_\mathrm{p}}{\partial X}=0$$

outlet plane, $X=L/D_\mathrm{i}$ $\quad 0<R<0.5\ \Rightarrow\ \frac{\partial W_X}{\partial X}=0,\ \frac{\partial W_R}{\partial X}=0,\ \frac{\partial\Theta_\mathrm{f}}{\partial X}=0$

$$0.5\le R\le R_\mathrm{w}\ \Rightarrow\ \frac{\partial\Theta_\mathrm{w}}{\partial X}=0$$

$$R_\mathrm{w}<R<R_\mathrm{o}\ \Rightarrow\ \frac{\partial\Theta_\mathrm{p}}{\partial X}=0$$

axe of symmetry, $R = 0$ $\quad 0 < X < L / D_{\mathrm{i}} \;\Rightarrow\; W_R = 0,\; \dfrac{\partial W_X}{\partial R} = 0,\; \dfrac{\partial \Theta_{\mathrm{f}}}{\partial R} = 0$

fluid – wall interface, $R = 0.5$ $\quad 0 < X < L / D_{\mathrm{i}} \;\Rightarrow W_X = W_R = 0,\; \left(\dfrac{\partial \Theta_{\mathrm{f}}}{\partial R}\right)_{R=0.5} = \dfrac{\lambda_{\mathrm{w}}}{\lambda_{\mathrm{f}}} \cdot \left(\dfrac{\partial \Theta_{w}}{\partial R}\right)_{R=0.5}$

wall – PCM interface, $R = R_{\mathrm{w}}$ $\quad 0 < X < L / D_{\mathrm{i}} \;\Rightarrow\; \left(\dfrac{\partial \Theta_{\mathrm{w}}}{\partial R}\right)_{R=R_{\mathrm{w}}} = \dfrac{\lambda_{\mathrm{p}}}{\lambda_{\mathrm{w}}} \cdot \left(\dfrac{\partial \Theta_{\mathrm{p}}}{\partial R}\right)_{R=R_{\mathrm{w}}}$

outer wall, $R = R_{\mathrm{o}}$ $\quad 0 < X < L / D_{\mathrm{i}} \;\Rightarrow\; \dfrac{\partial \Theta_{\mathrm{p}}}{\partial R} = 0\,.$

The governing differential equations of the HTF, the tube wall and the PCM, with initial and boundary conditions, have been solved as one domain. The computational domain has been discretised by the control volume approach and the SIMPLER algorithm. The formulation has been fully implicit in time and the convection-diffusion terms have been treated using power-law scheme. Algorithm has been implemented in developed FORTRAN computer code and the resulting discretisation equations have been solved simultaneously using an iterative procedure. Time-wise temperature distributions of HTF, tube wall and PCM have been obtained by numerical calculations and transient phase-change heat transfer behaviour during charging and discharging of the shell-and-tube thermal energy storage unit, i.e. melting and solidification of the PCM has been simulated.

EXPERIMENTAL INVESTIGATION AND NUMERICAL CODE VALIDATION

The numerical model has been validated with experimental data. An experimental vertical cylindrical latent thermal energy storage unit has been constructed and series of temperature measurements have been performed. Experimental test unit and thermocouples position inside the unit are shown in Fig. 2 and Fig. 3.

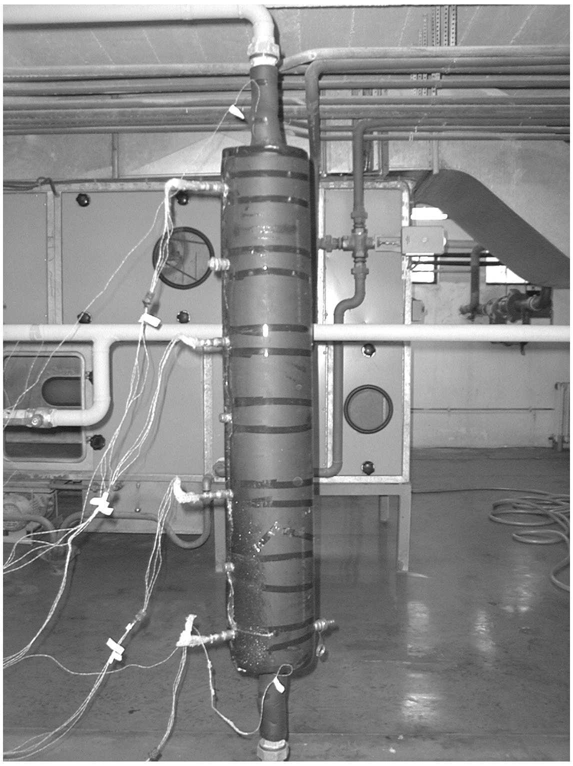

Fig. 2. Experimental test unit

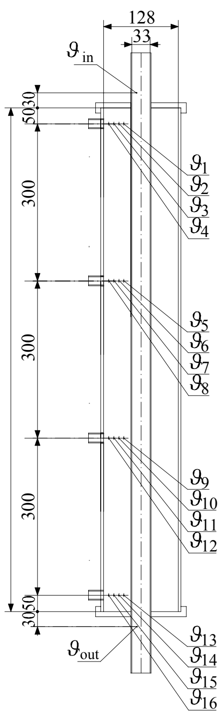

Fig. 3. Thermocuples position

An experimental test unit has been made of two concentric tubes, where the inside tube (0.033 m i.d., 0.035 m o.d. and 1 m length) has been made of copper, while the outside tube (0.128 m i.d., 0.133 m o.d. and 1 m length) has been made of brass. The outside tube has been well thermally insulated to reduce the heat losses. Sixteen K-type thermocouples have been placed inside the PCM at various locations. Two additional thermocouples have been placed at the inlet and outlet of the HTF into inside tube. All thermocouples have been connected to a data acquisition system. Labview commercial software has been used to record data in a database format on the personal computer. Temperature measurements have been recorded at a time intervals of 10 s. To maintain the axisymmetric melting around the inside tube, the test unit has been oriented in a vertical direction. Commercial paraffin Rubitherm RT 30, with thermophysical properties in Table 1, has been used in experimental studies as PCM, and water has been used as HTF.

Table 1. Thermophysical properties of the paraffin Rubitherm RT 30

Melting / solidification temperature	K	300.7
Latent heat capacity	kJ/kg	206
Thermal conductivity - solid / liquid	W/(mK)	0.18 / 0.19
Specific heat - solid / liquid	kJ/(kgK)	1.8 / 2.4
Density - solid / liquid	kg/m^3	789 / 750

Series of melting and solidification experiments has been performed for different mass flow rates and inlet temperatures of HTF. Computational model has been set up to reproduce these experimental conditions. Numerical calculations have been carried out for a grid size of 250 (axial) and 73 (radial) nodes, and dimensionless time steps of 0.06. In Figs. 4 and 5 paraffin temperature histories at locations 5 (x = 0.35 m; r = 0.0265 m) and 9 (x = 0.65 m; r = 0.0265 m) during melting, as well as at locations 2 (x = 0.05 m; r = 0.0355 m) and 15 (x = 0.95 m; r = 0.0445 m) during solidification are shown for both experiment and simulation. Mass flow rates and inlet temperatures of the HTF as well as initial temperatures of the PCM are indicated in figures.
The comparison between numerical predictions of time-wise temperature variations and experimental data shows a good agreement, although the natural convection in the liquid phase of the PCM has been ignored in the numerical model. It can be seen from Fig. 4 that melting of the applied PCM occurred non-isothermally over a certain temperature range within the melting zone. The shape of the temperature curves indicates that the melting dominates at about 27.7 to 35 ^{o}C. During solidification, paraffin has an isothermal phase change temperature range and no subcooling property, as shown in Fig. 5.

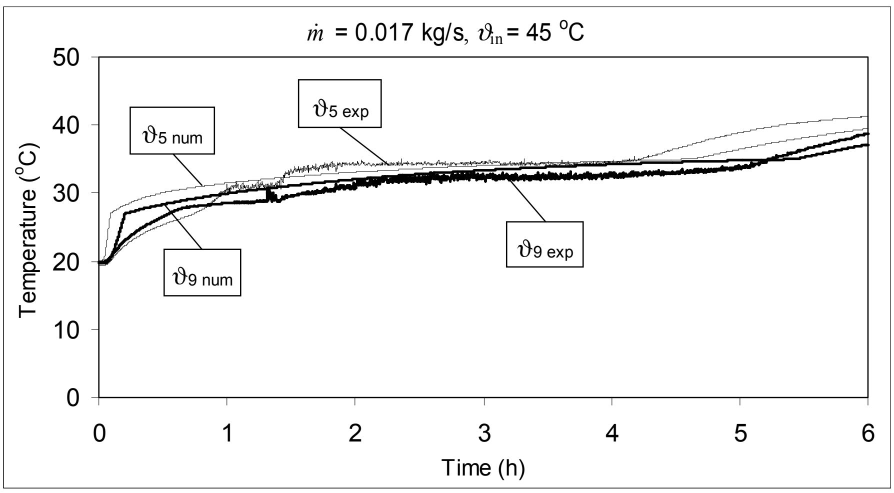

Fig. 4. Experimental and numerical time-wise PCM temperature variations during melting

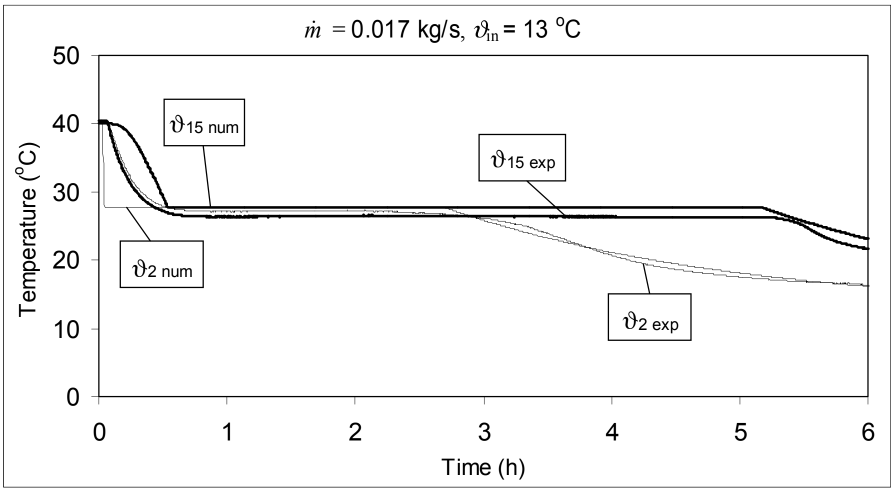

Fig. 5. Experimental and numerical time-wise PCM temperature variations during solidification

The results of analysis have signified that a developed numerical procedure could be efficiently used to simulate thermal behaviour of the latent thermal energy storage unit during charging and discharging.

NUMERICAL SIMULATION AND DISCUSSION

Series of numerical calculations have been carried out in order to analyse transient heat transfer during melting and solidification of the technical grade paraffin used in experimental investigations. Some of the computational results are illustrated further.

Fig. 6 shows radial dimensionless temperature distribution at an axial location of X = 12.73 in different dimensionless times during melting of PCM for laminar HTF flow with Re = 657. Melting of the PCM has occurred non-isothermally within a dimensionless temperature interval 0 to 0.42. The regions of HTF, tube wall and a PCM are indicated in the figure.

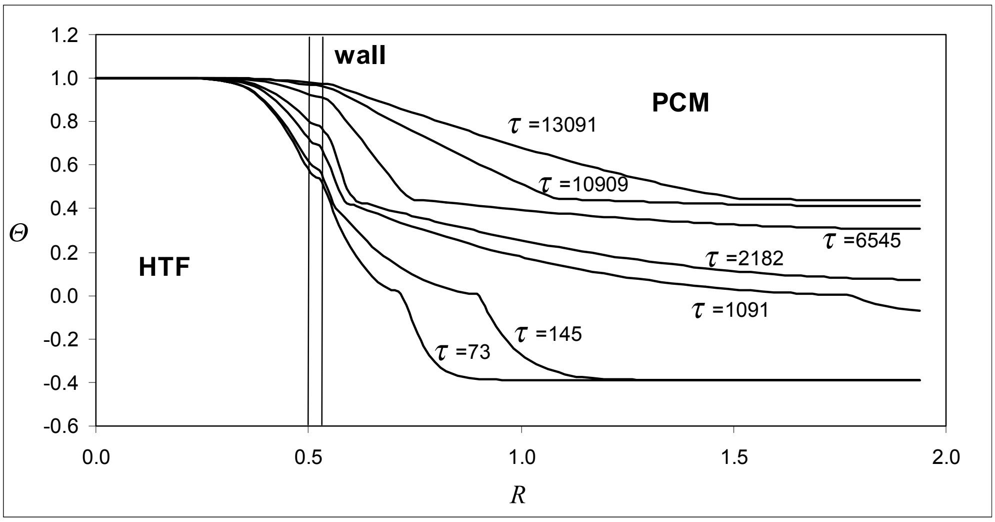

Fig. 6. Radial dimensionless temperature distribution at X = 12.73 in *different times during melting*

Melting of the paraffin starts on the HTF tube wall surface and expands inside the PCM storage tank. As melting front progresses, the temperature curve moves upward. The fluid velocity profile reaches a steady state quickly, while the temperature profile never reaches a fully developed state due to the moving melting front. This clearly approves that the use of empirical correlations for the convective heat transfer can result in a significant error.

Radial dimensionless temperature distribution at an axial location of X = 12.73 in different times during PCM solidification, for laminar HTF flow with Re = 657, is shown in Fig. 7. Solidification has occurred isothermally. Solidification fronts in different times are the intersections of the dimensionless temperature Θ = 0 and the corresponding temperature curves. Solidification of the PCM starts on the HTF tube wall surface and spreads inside PCM tank. Temperature curve moves downward due to a solidification front progression.

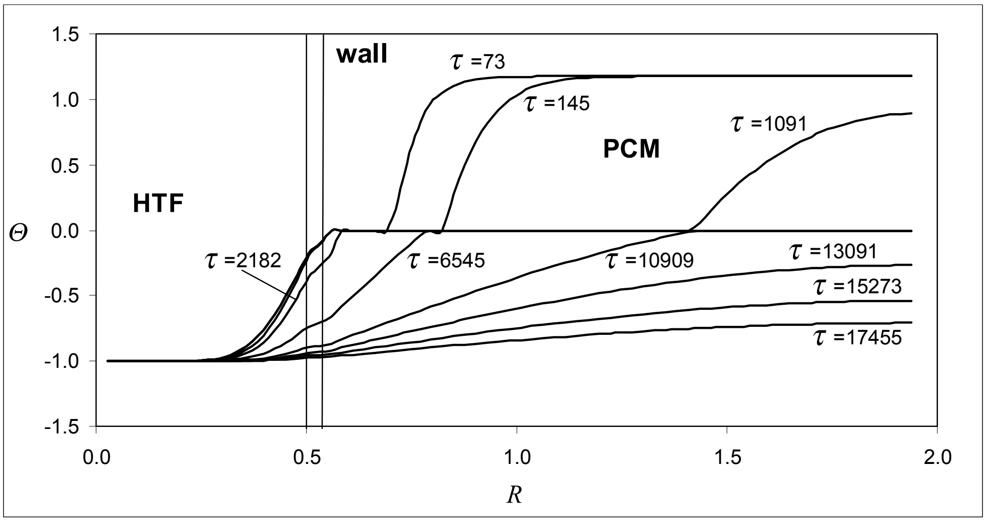

Fig. 7. Radial dimensionless temperature distribution at X = 12.73 in different times during solidification

The propagation of the solidification front is shown in Fig. 8. The solidification front moves in the axial direction of the PCM container faster than in the radial direction. Due to the relatively large Prandtl numbers (small thermal conductivity) of the water as HTF, a large amount of heat is carried downstream, while a relatively small amount of heat is transferred directly to the paraffin as PCM upstream. The solidification zones are indicated in the figure. At dimensionless time τ = 10909, the PCM is mainly in the solid phase.

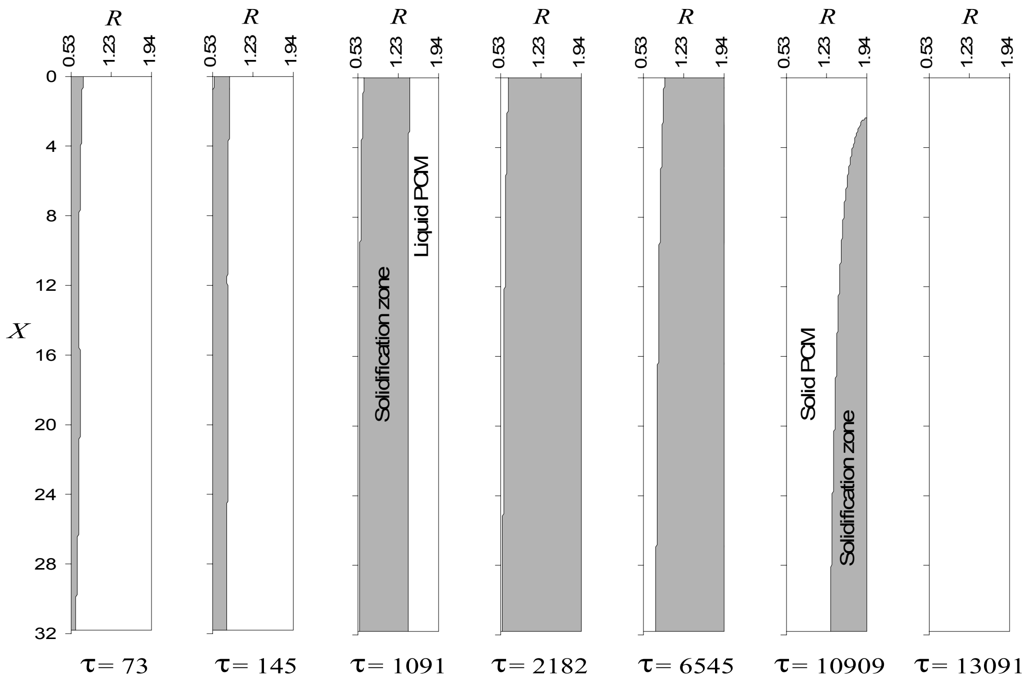

Fig. 8. Propagation of the solidification front

Spatial dimensionless temperature distributions of HTF, tube wall and PCM inside the latent storage unit in different times during PCM solidification are shown in Fig. 9.

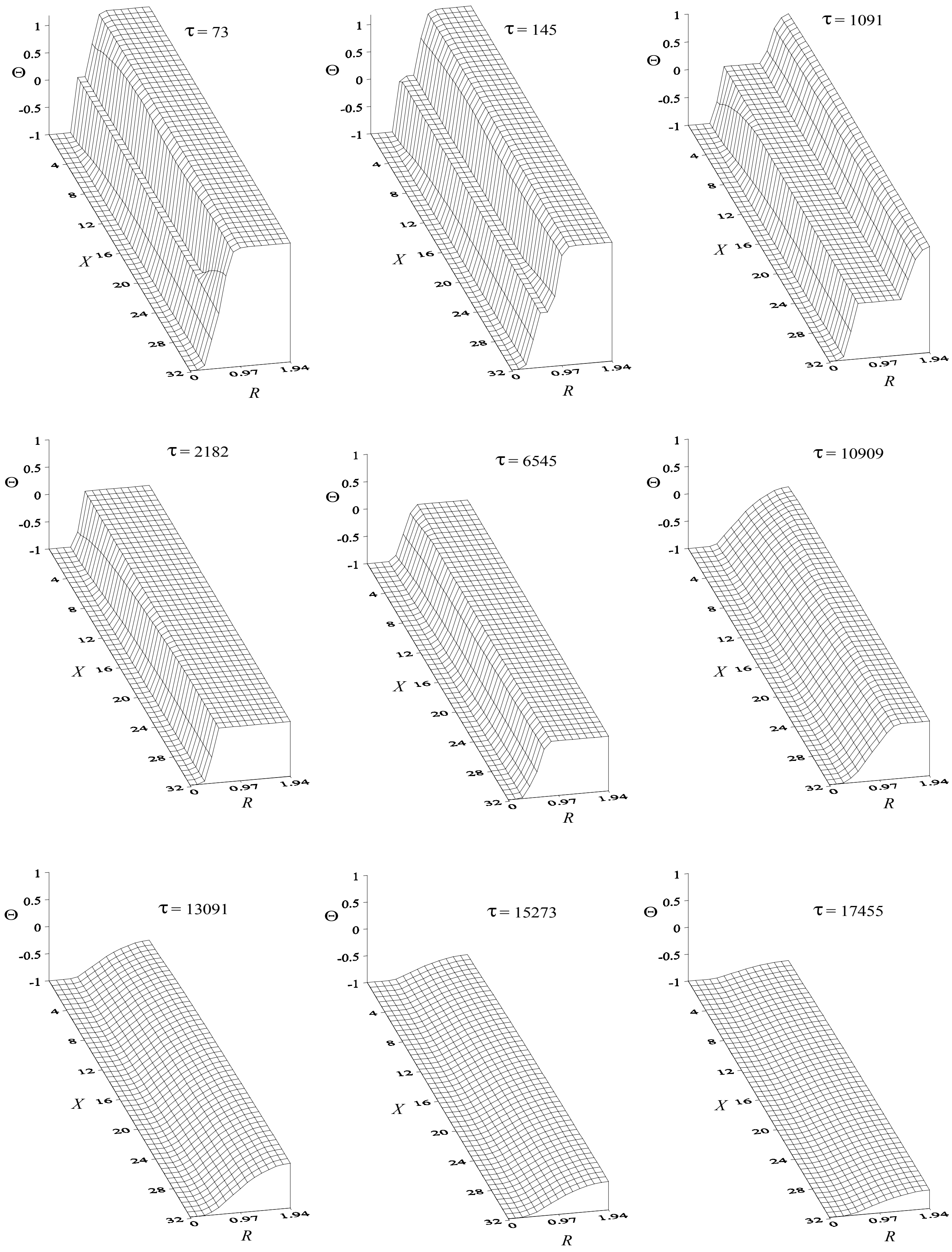

Fig. 9. Spatial dimensionless temperature distributions in different times during solidification

CONCLUSION

A numerical and experimental study of transient phase-change heat transfer during charging and discharging of the shell-and-tube latent thermal energy storage unit, with HTF circulating inside the tube and PCM filling the shell side, has been performed. Numerical predictions coincide quite well with the experimental results. Non-isothermal melting and isothermal solidification of technical grade paraffin, which has been used as PCM, have been observed by experimental investigations. Unsteady temperature distributions of HTF, tube wall and PCM have been calculated numerically. The results of numerical analysis underline that HTF velocities reach a steady state condition quickly, while temperatures change with moving of the melting/solidification interface, so it is necessary to treat the phase-change and fluid flow and heat transfer as a conjugate problem and solve them simultaneously as one domain. The usage of empirical correlations in expressing a convective heat transfer should be avoided. Due to the relatively large Prandtl numbers of the water as HTF, a large amount of heat is carried downstream, while a relatively small amount of heat is transferred directly to the paraffin as PCM upstream. The developed numerical procedure could be efficiently used for the simulation of transient thermal behaviour during charging and discharging of a latent thermal energy storage unit. Obtained numerical results provide guidelines for its design optimisation.

NOMENCLATURE

Symbols

a	thermal diffusivity, m^2/s
c	specific heat, J/(kgK)
D	diameter of the tube, m
H	volume enthalpy, J/m^3
L	length of the tube, m
$\dot{m}$	mass flow rate, kg/s
Nu	Nusselt number
P	dimensionless pressure
p	pressure, Pa
Pr	Prandtl number
q	latent heat capacity, J/kg
R	dimensionless coordinate along the radial direction
r	coordinate along the radial direction, m
Re	Reynolds number
St	Stefan number
T	thermodynamic temperature, K
t	time, s
W	dimensionless velocity
w	velocity, m/s
X	dimensionless coordinate along the axial direction
x	coordinate along the axial direction, m
α	convective heat transfer coefficient, $W/(m^2K)$
χ	dimensionless enthalpy
ϑ	temperature, °C
λ	thermal conductivity, W/(mK)
Θ	dimensionless temperature
ρ	density, kg/m^3
τ	dimensionless time
υ	kinematic viscosity, m^2/s

Subscripts

f	HTF
i	inside radius of the tube
in	inlet
init	initial
l	liquid phase of the PCM
m	melting / solification
o	outer surface of the latent storage unit
out	outlet
p	PCM
R	dimensionless coordinate along the radial direction
r	coordinate along the radial direction
s	solid phase of the PCM
w	wall
X	dimensionless coordinate along the axial direction
x	coordinate along the axial direction

REFERENCES

[1] Voller, V. R., Cross, M., Markatos, N. C.: *An Enthalpy Method for Convection/Diffusion Phase Change,* International Journal for Numerical Methods in Engineering, 24 (1987), 271-284.

[2] Voller, V. R.: *Fast Implicit Finite-Difference Method for the Analysis of Phase Change Problems,* Numerical Heat Transfer, 17 (1990), 155-169.

[3] Hunter, L. W., Kuttler, J. R.: *The Enthalpy Method for Heat Conduction Problems With Moving Boundaries,* Journal of Heat Transfer, 111 (1989), 239-242.

[4] Cao, Y., Faghri, A., Chang, W. S.: *A numerical analysis of Stefan problems for generalized multi-dimensional phase-change structures using the enthalpy transforming model*, International Journal of Heat and Mass Transfer, 32 (1989) 7, 1289-1298.

[5] Lee, S. L., Tzong, R. Y.: *An Enthalpy Formulation for Phase Change Problems with a Large Thermal Diffusivity Jump Across the Interface,* International Journal of Heat and Mass Transfer, 34 (1991) 6, 1491-1502.

[6] Bellecci, C., Conti, M.: *Phase change thermal storage: transient behaviour analysis of a solar receiver / storage module using the enthalpy method*, International Journal of Heat and Mass Transfer, 36 (1993) 8, 2157-2163.

[7] Bellecci, C., Conti, M.: *Latent heat thermal storage for solar dynamic power generation*, Solar Energy, 51 (1993) 3, 169-173.

[8] Bellecci, C., Conti, M.: *Transient behaviour analysis of a latent heat thermal storage module*, International Journal of Heat and Mass Transfer, 36 (1993) 15, 3851-3857.

[9] Lacroix, M.: *Numerical Simulation of a Shell-and-tube Latent Heat Thermal Energy Storage Unit,* Solar Energy, 50 (1993) 4, 357-367.

[10] Lacroix, M.: *Study of the heat transfer behaviour of a latent heat thermal energy storage unit with a finned tube*, International Journal of Heat and Mass Transfer, 36 (1993) 8, 2083-2092.

[11] Cao, Y., Faghri, A.: *Performance characteristics of a thermal energy storage module: a transient PCM / forced convection conjugate analysis*, International Journal of Heat and Mass Transfer, 34 (1991) 1, 93-101.

[12] Cao, Y., Faghri, A.: *A Study of Thermal Energy Storage Systems With Conjugate Turbulent Forced Convection*, Journal of Heat Transfer, 114 (1992), 1019-1027.

[13] Ismail, K. A. R., Abugderah, M. M.: *Performance of a thermal storage system of the vertical tube type*, Energy Conversion & Management 41 (2000), 1165-1190.

[14] Zhang, Y., Faghri, A.: *Semi-analytical solution of thermal energy storage system with conjugate laminar forced convection*, International Journal of Heat and Mass Transfer, 39 (1996) 4, 717-724.

[15] Trp, A., Frankovic, B., Lenic, K.: *An Analysis of Phase Change Heat Transfer in a Solar Thermal Energy Store,* Proceedings of the ISES 1999 Solar World Congress, Vol. III, Jerusalem, Israel, 1999, 484-489.

[16] Farid, M. M., Khudhair, A. M., Razack, S. A. K., Al-Hallaj, S.,: *A review on phase change energy storage: materials and applications*, Energy Conversion and Management 45 (2004), 1597-1615.

[17] Patankar, S. V.: *Numerical Heat Transfer and Fluid Flow,* Hemisphere Publishing Corporation, Taylor & Francis Group, New York, 1980.

[18] Versteeg, H. K., Malalasekera, W.: *An Introduction to Computational Fluid Dynamics: The Finite Volume Method,* Longman Scientific & Technical, Essex, 1995.